PORTLAND
PRESS

Research Article

Fatty acid oxidation inhibitor etomoxir suppresses tumor progression and induces cell cycle arrest via PPARγ-mediated pathway in bladder cancer

Songtao Cheng[1,*], Gang Wang[2,3,4,*], Yejinpeng Wang[1], Liwei Cai[5], Kaiyu Qian[2,3], Lingao Ju[2,3], Xuefeng Liu[6], Yu Xiao[1,2,3,4] and Xinghuan Wang[1,7,8]

[1]Department of Urology, Zhongnan Hospital of Wuhan University, Wuhan, China; [2]Department of Biological Repositories, Zhongnan Hospital of Wuhan University, Wuhan, China; [3]Human Genetics Resource Preservation Center of Hubei Province, Wuhan, China; [4]Laboratory of Precision Medicine, Zhongnan Hospital of Wuhan University, Wuhan, China; [5]Department of Medicine, Nanchang University, Nanchang, China; [6]Department of Pathology, Lombardi Comprehensive Cancer Center, Georgetown University Medical School, Washington DC, U.S.A.; [7]Medical Research Institute, Wuhan University, Wuhan, China; [8]Urological Clinical Research Center of Laparoscopy in Hubei Province, Wuhan, China

Correspondence: Gang Wang (gangwang.uro@whu.edu.cn) or Xinghuan Wang (wangxinghuan@whu.edu.cn)

OPEN ACCESS

Tumor cells rely on aerobic glycolysis as their main energy resource (Warburg effect). Recent research has highlighted the importance of lipid metabolism in tumor progression, and certain cancers even turn to fatty acids as the main fuel. Related studies have identified alterations of fatty acid metabolism in human bladder cancer (BCa). Our microarray analysis showed that fatty acid metabolism was activated in BCa compared with normal bladder. The free fatty acid (FFA) level was also increased in BCa compared with paracancerous tissues. Inhibition of fatty acid oxidation (FAO) with etomoxir caused lipid accumulation, decreased adenosine triphosphate (ATP) and nicotinamide adenine dinucleotide phosphate (NADPH) levels, suppressed BCa cell growth *in vitro* and *in vivo*, and reduced motility of BCa cells via affecting epithelial–mesenchymal transition (EMT)-related proteins. Furthermore, etomoxir induced BCa cell cycle arrest at G_0/G_1 phase through peroxisome proliferator-activated receptor (PPAR) γ-mediated pathway with alterations in fatty acid metabolism associated gene expression. The cell cycle arrest could be reversed by PPARγ antagonist GW9662. Taken together, our results suggest that inhibition of FAO with etomoxir may provide a novel avenue to investigate new therapeutic approaches to human BCa.

Introduction

Bladder cancer (BCa), currently the ninth most common cause of cancer with a gradually increasing global incidence in the last 30 years, is relatively common in more developed areas and occurs more frequently among males than females (sex ratio worldwide of 3.5:1) [1]. As one of the most common malignances in the urinary system, 70% of newly diagnosed patients are non-muscle-invasive BCa (NMIBC) [2], which is treated by transurethral resection, followed by intravesical instillations of immunotherapy or chemotherapy [3]. At the present stage, the gold standard therapeutic method for muscle-invasive BCa (MIBC) is radical cystectomy, which still has many unfavorable outcomes [4,5]. However, even after receiving radical cystectomy, the BCa recurrence and distant metastasis rate remains approximately 50%, and its 5-year survival rate is only 50–66% [6–8]. Therefore, more effective therapeutic strategies need to be detected for BCa treatment.

Reprogramming of energy metabolism has been recognized as a hallmark of cancer [9,10]. Otto Warburg first described that cancer cells prefer aerobic glycolysis as the main energy resource even when oxygen is sufficient, which is known as the Warburg effect [11–13]. However, recent studies have stressed the crucial role of fatty acid oxidation (FAO) in providing adenosine triphosphate (ATP), nicotinamide adenine dinucleotide phosphate (NADPH), and other important anabolic materials in cancer cells [14–16].
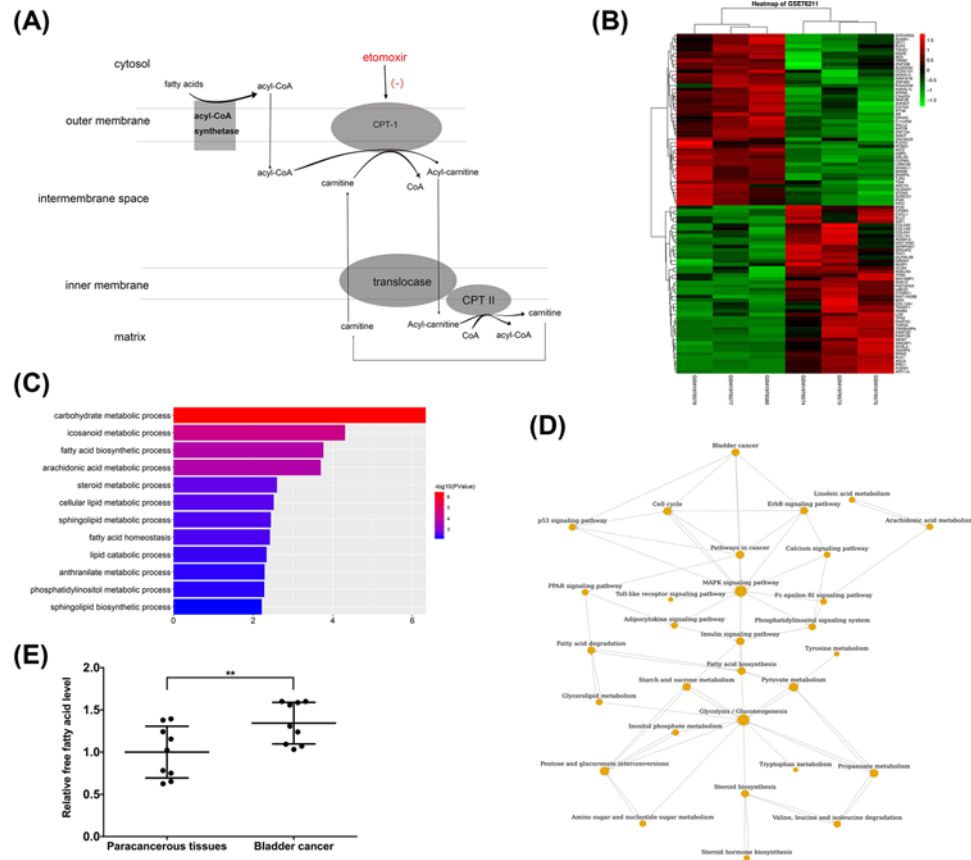
Figure 1. Altered fatty acids metabolism in BCa

(**A**) Etomoxir could inhibit fatty acids transportation into mitochondrion. (**B**) Heat map of the top 50 DEGs in BCa compared with normal bladder tissues. Red represents up-regulation and green represents down-regulation. (**C**) Enrichment of functions of DEGs revealed a strong relation with fatty acid metabolism and lipid catabolic process. (**D**) GO-map network analysis indicated that glycerolipid metabolism and fatty acid degradation were linked with BCa through PPAR signaling pathway, and cell cycle was closely related to BCa. (**E**) FFA level in BCa was higher than in paired paracancerous tissues ($n=9$). **$P<0.01$. Abbreviations: DEG, differentially expressed gene; FFA, free fatty acid; GO, gene ontology.

Lin et al. [17] reported that FAO was active in glioma tissues and inhibition of FAO with etomoxir reduced energy production and cell proliferation. Furthermore, some kind of cancers rely on lipid fuel more than on aerobic glycolysis [18], which is greatly different from the Warburg effect. Recent studies showed that alterations in lipid metabolism were attached to bladder carcinogenesis [19]. As some metabolomics profiling analysis showed [20], there may exist an active fatty acid β-oxidation in promoting development and progression of BCa.

To be fully oxidized, fatty acids, derived from fatty acid synthesis (FAS) or extracellular environment, with the assistance of fatty acid binding proteins (FABP), are located at the outer membrane of mitochondria and then activated to fatty acyl-CoAs by fatty acyl-CoA synthetase. For the lack of permeability to the inner mitochondrial membrane, long-chain acyl-CoA is converted into acylcarnitine catalyzed by carnitine palmitoyltransferase I (CPT1), which is the first rate-limiting step of FAO [21]. Then, acylcarnitine is transported by carnitine acylcarnitine translocase (CACT) and converted back into acyl-CoA by carnitine palmitoyltransferase II (CPT2) in mitochondrial matrix for subsequent oxidation [22]. The most prominent regulators of FAO are peroxisome proliferator-activated receptors (PPARs), consisting of three isoforms PPARα, PPARβ/δ and PPARγ. Expressed in various tissues at different levels, they have different functions with partial overlapping. By regulating gene expression and biological processes associated with lipid metabolism [23,24], they are critical in modulating FAO.

Etomoxir is an irreversible inhibitor of CPT1 and has been clinically used for chronic heart failure and type 2 diabetes mellitus for a long time [25,26], but retired due to its adverse side effects in the liver [27]. Figure 1A illustrated

part of the process by which fatty acids were transported into mitochondria for subsequent β-oxidation and the inhibitory site of etomoxir. Pharmacological inhibition of FAO with etomoxir was mostly used in research, and some recent experiments indicated promising anti-tumor results [28,29]. But studies reported that the effects of etomoxir on tumor growth are still not adequate, and there are no such studies published in BCa. In our study, we investigated the effects of FAO inhibition with etomoxir in BCa cell viability, fatty acid metabolism, motility,and molecular mechanisms. Our results indicated that FAO, inhibited by etomoxir in BCa cells, is important in sustaining tumor growth, decreasing cell migration and invasion, and inducing cell cycle arrest at G_0/G_1 phase through PPARγ-mediated pathway. Inhibition of FAO with etomoxir may provide a novel avenue to investigate new therapeutic approaches to human BCa.

Materials and methods

BCa cell lines

Human BCa cell lines UM-UC-3 (Cat. #TCHu217) and T24 (transitional cell carcinoma, Cat. #SCSP-536) were obtained from Chinese Academy of Sciences in Shanghai, China. The cell lines were authenticated by the China Center for Type Culture Collection in Wuhan. UM-UC-3 cells were maintained in DMEM (Gibco) and T24 cells were maintained in RPMI-1640 medium (Gibco) supplemented with 10% fetal bovine serum (FBS) in a humidified atmosphere composed of 5% CO_2 and 95% air at 37°C. All human cell lines authenticated using STR profiling within the last 3 years have been included. All experiments were performed with mycoplasma-free cells.

Drug treatment of BCa cells

MTT assay of etomoxir treatment

A total of 3000 BCa cells in 200 μl medium were pipetted into 96-well plates to grow for 24 h, and then treated by etomoxir (Sigma–Aldrich, Cat. #E1905) (0, 25, 50, 75, 100, 150, and 200 μM, diluted in pure water) or ST1326 (Avanti, Cat. 870853P) (0, 0.1, 0.5, 1, 5, 10, 25, and 50 μM, diluted in phosphate buffer saline) for 24, 48, and 72 h. After adding 20 μl MTT in each well, incubating 4 h at 37°C, discarding the medium and dissolving formazan precipitate in 150 μl DMSO, the absorbance at 490 nm was detected by a microplate reader (Molecular Devices, Cat. #SpectraMax M2). And the following experiments of etomoxir-treated BCa cells were generated as follows: cells were first cultured for 24 h and then treated by etomoxir at 0, 75, and 150 μM for 48 h.

Pretreatment of PPARγ antagonist for rescue experiments

BCa cells were first incubated for 24 h and subsequently treated with PPARγ antagonist GW9662 (Sigma–Aldrich, Cat. #M6191) at final concentrations of 0, 20, and 40 μM for 24 h. Next, cells were treated by etomoxir for another 48 h and then collected for relevant experiments. GW9662 was initially dissolved in DMSO as stock solution with a concentration of 50 mM, and the 0 μM group added DMSO to a concentration of 0.1% as control.

RNA expression analyses

Total RNA isolation

Total RNA was extracted from BCa cells and bladder tissues using the Qiagen RNeasy Mini Kit (Qiagen, Cat. #74101) and QIAshredder from Qiagen (Qiagen, Cat. #79654) according to the manufacturer's instructions. Genomic DNA contamination was removed with DNase I digestion (Qiagen, Cat. #79254) in each RNA sample. The quantity control of isolated RNA was assessed by NanoDrop® ND-2000 UV-Vis spectrophotometer (Thermo Scientific).

Microarray analysis

Microarray analysis was proceeded as previously described [31]. Briefly, according to standard Affymetrix protocol, biotinylated cDNA was prepared from 250 ng extracted RNA with Ambion® WT Expression Kit. And then, 5.5 μg cDNA was hybridized, washed, stained, and scanned. Data were processed and analyzed with Gene Ontology (GO) and Kyoto Encyclopedia of Genes and Genomes (KEGG) pathway. The microarray data of bladder tissues were submitted to the Gene Expression Omnibus (GEO) database and the accession number is GSE76211. All data were MIAME compliant.

Reverse transcription and quantitative real-time PCR

The cDNA was synthesized from 1 μg of total RNA with RevertAid Ace qPCR RT kit (Toyobo). Then 1 μg cDNA was added in each reaction to a final volume of 20 μl with iQ™ SYBR®-Green Supermix (Bio-Rad). All primer sequences

with its annealing temperatures were listed in Supplementary Table S1. And the cycle numbers of threshold (C_T) values were normalized to GAPDH.

Free fatty acid, ATP and NADPH assay

Free fatty acid (FFA) level of tissues and cells was measured by Free Fatty Acid Quantitation Kit (Sigma–Aldrich, Cat. #MAK044). The ATP and NADPH level were determined using ATP Assay Kit (Beyotime, Cat. #S0026) and NADP/NADPH Quantification Colorimetric Kit (Biovision, Cat. #K347-100), respectively. All the procedures were performed according to the manufacturers' instructions.

Gas chromatography-flame ionization detection

Cell samples were homogenized individually with 5% concentrated sulfuric acid methanol and 0.2% butylated hydroxytoluene methanol in ice water bath for ultrasonic for 15 min. After mixing and extracting in a constant temperature water bath at 90–95°C for 1.5 h, cooling to room temperature, saturated NaCl and n-hexane were added to vortex for 1 min. Then the following steps were performed: centrifuging at 5 min, 4°C, 3500 rpm, transferring supernatants to a new centrifuge tube, and vortexing with nonadecanoic acid methyl ester for 10 s. Then fatty acids were identified and quantified by 7890A GC-5975C FID (Agilent, U.S.A.) with an Agilent DB-225 capillary column (10 m × 0.1 mm i.d., 0.1 μm film thickness). The carrier gas was helium. The initial temperature of column was set at 50°C, then increased to 205°C at a rate of 30°C/min, held for 1 min, increased again to 230°C, and then held isothermally. The inlet and FID temperature was 250°C, and the split ratio was 1:15. All the data were analyzed and processed with FID Chem Station (G1701EA.02.00.493) and ACD/Spectrus Processor 2015 (S30S41) software.

Cell culture experiment

Oil Red O staining

Etomoxir-treated BCa cells were fixed with paraformaldehyde (PFA) for 15 min, rinsed in distilled water and 60% isopropanol, and stained with freshly prepared Oil Red O (Sigma–Aldrich, Cat. #SLBP5248V) working solution for 10 min at room temperature. Then cell slides were rinsed with 60% isopropanol and distilled water, counterstained with Hematoxylin (Sigma–Aldrich, Cat. #H9627), mounted in glycerol gelatin medium and observed with a phase contrast microscope (Leica, Cat. #DMI 1).

Clonogenic survival assay

A total of 800 UM-UC-3 cells/well and 1000 T24 cells/well were added in six-well plates to grow into colonies for 7–10 days. The medium was removed, the cells were fixed with 4% PFA, then stained with Crystal Violet for 30 min, followed by photographing and counting.

Flow cytometry analysis

After collecting and washing with cold PBS, BCa cells were resuspended with 1× DNA Staining Solution containing permeabilization solution and propidium iodide (Multi sciences), then incubated in the dark for 30 min at 37°C. Flow cytometry (Beckman, Cat. #FC500) was used to analyze the cell cycle. According to its manufacturer's instructions, cell apoptosis analysis was conducted using annexin V-fluorescence isothiocyanate (FITC)/PI apoptosis detection kit (BD biosciences) by flow cytometry.

Wound healing assay

Cells were cultured in six-well plates and scratched with a tip, washed with PBS. Medium containing different concentrations of etomoxir was added and results were photographed by a phase contrast microscope in several pre-marked spots at 0 and 12 h. The rate of migration was analyzed statistically.

Transwell chamber assay

A total of 4×10^4 BCa cells in 200 μl serum-free medium were seeded in the upper transwell chamber (Corning), with 600 μl medium containing 10% FBS in the lower chamber to induce cell migration. After incubation for 24 h at 37°C, removing the cells in the upper chamber, fixing and staining with 0.1% Crystal Violet, then photographing and counting migrated cells by phase contrast microscope. To conduct invasion assay, the transwell chambers were percolated with ECM Matrix gel solution (Sigma–Aldrich) for 1 h at 37°C, and 1×10^5 cells were seeded as described previously. Subsequent procedures were the same as those of the migration assays.

Protein analyses

Western blot analysis

BCa cells were lysed and sonicated on ice in RIPA buffer including protease inhibitor (Sigma–Aldrich) and phosphatase inhibitor for approximately 30 min. Then after centrifuging at $12000 \times \boldsymbol{g}$ for 10–15 min, the supernatant was collected. Protein was separated using 7.5–12.5% SDS/PAGE gels and transferred to the PVDF membrane (Millipore), which was then blocked in 5% fat-free milk (BD Biosciences) and incubated with primary antibodies (Supplementary Table S2) overnight and secondary antibodies (Supplementary Table S3) for 2 h. Bands were detected by enhanced chemiluminescence kit (Bio-Rad) and visualized by Molecular Imager Chemi Doc XRS$^+$ Imaging system (Bio-Rad).

Enzyme-linked immunosorbent assay

PPARγ and PPARα DNA-binding activity was detected using PPARγ and PPARα transcription factor assay kit (Abcam) independently according to the manufacturer's instructions. Briefly, the nuclear fraction was prepared from BCa cells using Nuclear and Cytoplasmic Extraction Reagents (Thermo Scientific). Then, conjunction of primary and secondary antibodies was conducted according to the protocols. The absorbance at 450 nm was detected by a microplate reader (Molecular Devices, Cat. #SpectraMax M2).

Immunofluorescence and immunohistochemistry staining

Immunofluorescence staining of BCa cells was previously described [31]. For immunohistochemistry (IHC) staining, paraffin sections from xenograft tumors were deparaffinized. Then antigen retrieval was conducted in citrate buffer. Inactivating endogenous peroxidase activity in 0.3% H_2O_2 and blocking in goat serum for another 30 min, the section was subsequently incubated in the indicated primary and secondary antibodies. After counterstaining with Hematoxylin, the slices were eventually visualized by Olympus BX53 biological microscope.

Hematoxylin and Eosin staining

All the tissue paraffin sections from xenograft tumors were stained with Hematoxylin and Eosin (H&E). The slides were serially deparaffinized, rehydrated by xylene, 100% ethanol, 96% ethanol, 80% ethanol, 70% ethanol, and H_2O. Sections were subsequently stained with 10% Hematoxylin (Sigma–Aldrich) for 7 min. And 1% Eosin (Sigma–Aldrich) with 0.2% glacial acetic acid was taken to stain the cytoplasm. Images of the slices were eventually taken by an inverted phase contrast microscope (Leica, Cat. #DMI 1).

Xenograft mouse model

Male BALB/c nude mice (3 weeks old) were obtained from Beijing HFK Bioscience Co., Ltd. in Beijing, China. After adaptation of 1 week in the laboratory of animal facility of Zhongnan Hospital of Wuhan University, mice were injected with T24 cells of 3×10^6 dispersed in 0.2 ml PBS into the right flank. Twelve days later, mice with approximately 3 mm × 3 mm tumors were assigned to two groups ($n=5$) randomly. Etomoxir (40 mg/kg) and vehicle were injected intraperitoneally every other day for 20 days. The tumor size was measured every 2 days and calculated as: tumor volume (mm^3) = length × width^2 × 0.5. After killiing, tumor tissues were dissected for tumor weight and fixed in 4% PFA preparing for subsequent staining. Animal experiment complied with the ARRIVE guidelines and carried out according to the U.K. Animals (Scientific Procedures) Act, 1986 and associated guidelines, EU Directive 2010/63/EU for animal experiments. The animal experiment was approved by the Institutional Animal Care and Use Committee at Center for Animal Experiment, Wuhan University (approval no. 2018152).

Statistics

All experiments were performed at least three times, and representative data were from three iterations. One-way analysis of variance (ANOVA) and two-tailed Student's t test were used to evaluate statistical significance of differences between subgroups. All the statistical analyses were conducted with SPSS 16.0, and the cut-off level was set at probability values of $P<0.05$.

Results

Fatty acids metabolism was altered in BCa tissues

The differentially expressed genes (DEGs) were detected in three MIBC tissues compared with three normal bladder tissues by microarray (Figure 1B). GO analysis revealed that DEGs were associated with a variety of metabolic process especially the fatty acid metabolic process (Figure 1C). Path-net analysis based on KEGG pathway in GCBI platform showed that fatty acid degradation, cell cycle, PPAR signaling pathway, and p53 signaling pathway were significantly
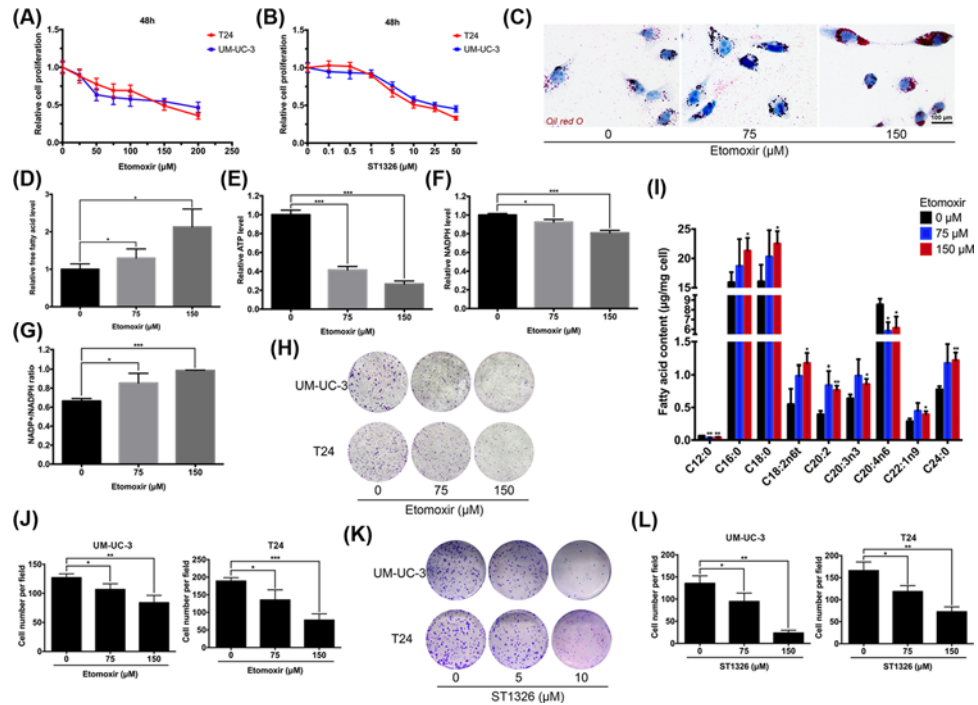
Figure 2. FAO inhibition of etomoxir in BCa

MTT assay was used to test the viability of cells treated with etomoxir (**A**) and ST1326 (**B**) at different concentrations. (**C**) Increased lipid accumulation and (**D**) elevated FFA level was caused by etomoxir in BCa UM-UC-3 cells. The (**E**) ATP and (**F**) NADPH levels were decreased, and (**G**) NADP$^+$/NADPH ratio was increased in UM-UC-3 cells. (**H**) The influence of etomoxir on cell survival was detected by clonogenic survival assay, (**I**) and alterations of fatty acid content were detected by GC-FID. (**J**) Statistical analysis of (**H**). (**K**) Clonogenic survival assay was performed to detect the influence of ST1326 on BCa cells, (**L**) confirmed by statistical analysis. Cell types and drug concentrations are indicated. Representative images were from three iterations. *$P<0.05$, **$P<0.01$, ***$P<0.001$.

related to BCa (Figure 1D). We detected the FFA levels in nine pairs of BCa tissues and paracancerous tissues, and found that there were significantly increased FFA levels in BCa tissues (Figure 1E). To verify if the genes involved in metabolism were misregulated, quantitative real-time PCR (qRT-PCR) was performed in paired BCa and paracancerous tissues. Although the alteration of CPT1A gene expression in BCa tissues was not significant, our results showed that ACSL1, SCD1, CD36, and PLA2 were up-regulated, while ACAD7 and PTGIS were down-regulated in BCa compared with paracancerous tissues (Supplementary Figure S1A–G). Taken together, we hypothesized that fatty acids catabolism was altered in BCa, and inhibition of fatty acids oxidation might have a great impact on BCa (Figure 1A).

FAO inhibition by etomoxir reduced proliferation of BCa cells

We treated BCa cells with etomoxir and ST1326 at different concentrations (0, 25, 50, 75, 100, 150, 200 μM and 0, 0.1, 0.5, 1, 5, 10, 25, 50 μM, respectively) for 24, 48, and 72 h (Figure 2A,B and Supplementary Figure S1H–K), and found that etomoxir and ST1326 could inhibit UM-UC-3 and T24 cell viability in a dose-dependent manner. Based on the MTT assay, in the following experiments, cells were treated with etomoxir at 75 and 150 μM for 48 h as the low- and high-dose groups and vehicle as the control group for subsequent tests. Oil Red O staining revealed that lipid accumulation was increased in etomoxir-treated UM-UC-3 cell (Figure 2C). Consistently, etomoxir treatment increased the FFA level in UM-UC-3 cell (Figure 2D). Compared with fatty acid standard by gas chromatography-flame ionization detection (GC-FID), the absolute qualitative and quantitative analysis of fatty acid composition was conducted in etomoxir-treated UM-UC-3 cells (Supplementary Figure S1L–M). Fatty acids, such as C16:0, C18:0, C18:2n6t, C20:2, C20:3n3, C22:1n9, and C24:0 were significantly elevated, while C12:0 and C20:4n6 were decreased in UM-UC-3 cells caused by the FAO inhibition of etomoxir (Figure 2I).
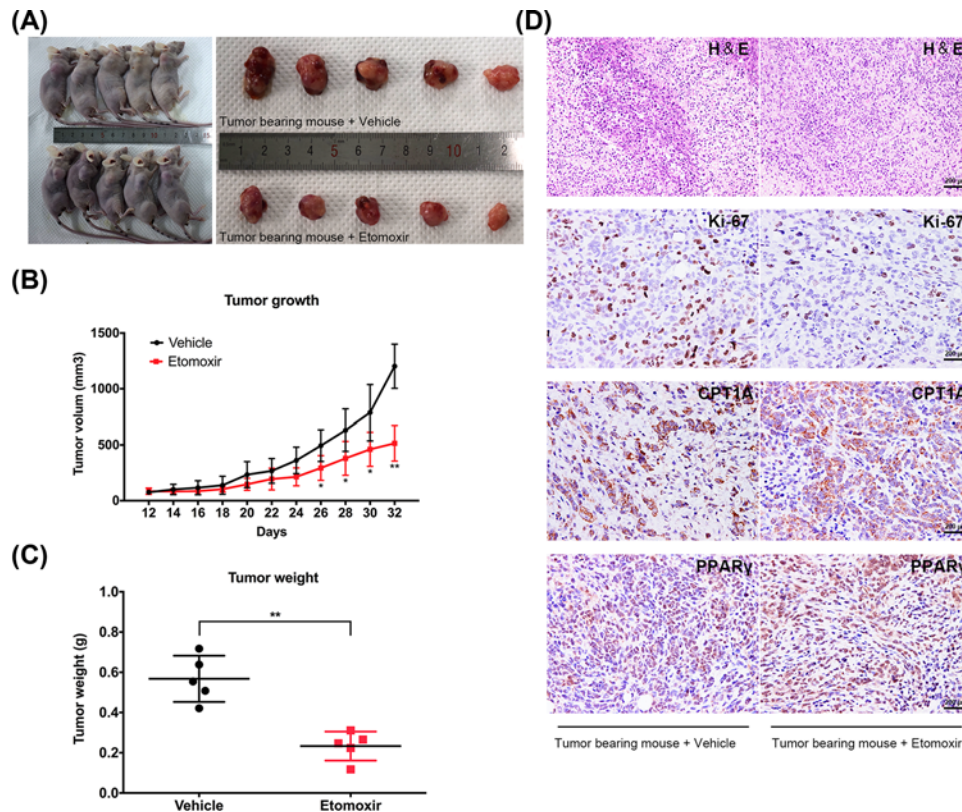
Figure 3. Etomoxir inhibited BCa growth *in vivo*
(**A**) BALB/c nude mice were subcutaneously injected with T24 cells to grow for 12 days. Then etomoxir and vehicle were intraperitoneally injected every other day for additional 20 days. (**B**) Tumor volume was calculated before each injection. After killing, tumor tissues were dissected from mice. (**C**) Tumor weight in vehicle group was higher than in etomoxir group. *$P<0.05$, **$P<0.01$. (**D**) Representative H&E and IHC staining of dissected tumor tissues showed the down-regulated Ki-67, up-regulated PPARγ and unchanged CPT1A in the etomoxir group compared with the vehicle group. The scale bars were indicated.

To further confirm the FAO inhibition of etomoxir, we detected the ATP and NADPH level in BCa UM-UC-3 cells, and found that ATP and NADPH level were significantly decreased in etomoxir treated groups (Figure 2E,F) and $NADP^+/NADPH$ ratio was increased (Figure 2G). By inhibition of FAO, the proliferation inhibitory effect of etomoxir and ST1326 was validated with clonogenic survival assay (Figure 2H,K), and confirmed by statistical analysis (Figure 2J,L), respectively.

Etomoxir suppressed BCa cell growth *in vivo*

We established a mouse model by transplanting T24 cells subcutaneously to further evaluate the effect of etomoxir on BCa cell growth *in vivo* (Figure 3A). The results indicated that etomoxir could significantly suppress tumor growth compared with the vehicle group (Figure 3B). After the indicated time, all tumors were dissected from the mice, and the tumor weight of etomoxir treatment group was lower in comparison with the vehicle group (Figure 3C). The tumor tissues dissected from mice were stained with H&E, and the IHC staining analysis results showed that Ki-67, an important marker of cell proliferation [32], was considerably decreased in the etomoxir-injected group (Figure 3D). Moreover, the positive staining of PPARγ was up-regulated in etomoxir group compared with the vehicle group, but the alteration of CPT1A was not significant between the two groups (Figure 3D).

Etomoxir induced cell cycle arrest and motility inhibition in BCa cells

The flow cytometry analysis indicated that the cell cycle was arrested at G_0/G_1 phase in etomoxir-treated BCa UM-UC-3 (Figure 4A) and T24 cells (Supplementary Figure S2A) in a dose-dependent manner. However, we did not observe significant apoptosis even in the high concentration group in UM-UC-3 cells (Figure 4B), as well as
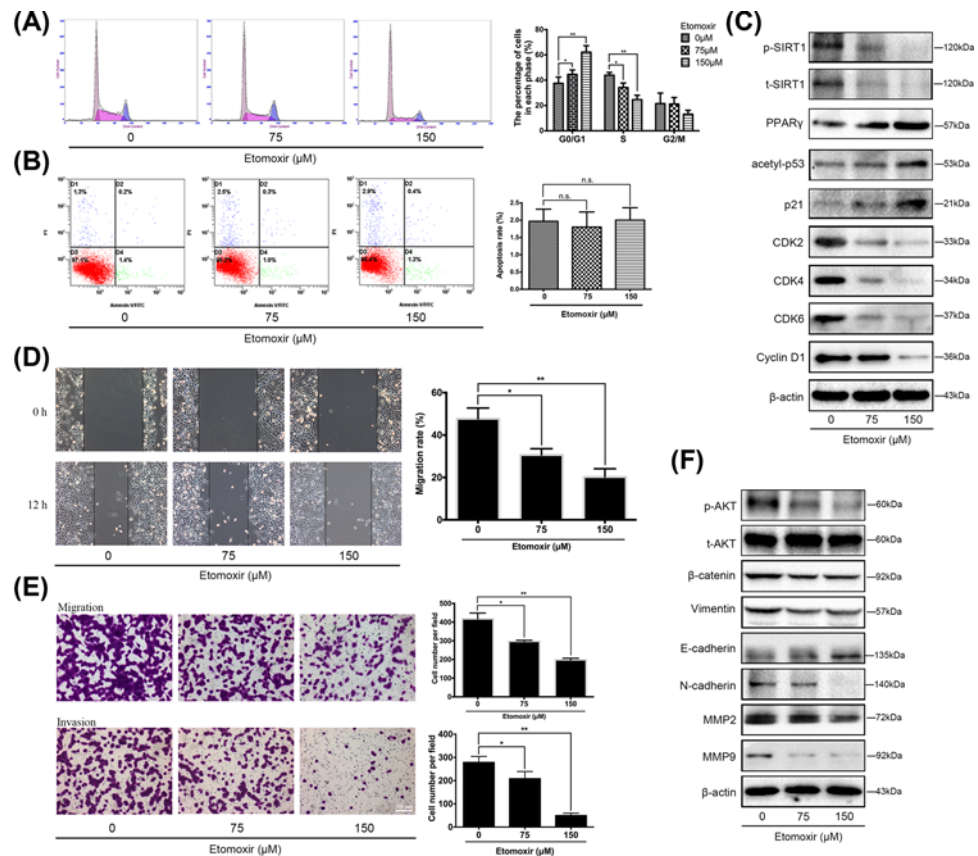
Figure 4. Cell cycle and motility were inhibited by etomoxir in UM-UC-3

Flow cytometry analysis of cell cycle (**A**) and apoptosis (**B**). G_0/G_1 related proteins and upstream indicator were validated by WB analysis. PPARγ signaling pathway related proteins such as PPARγ was up-regulated, and phosphorylated and total SIRT1 were down-regulated (**C**). (**D**) Wound healing assay and (**E**) transwell migration and invasion assay of UM-UC-3 cells treated with different concentrations of etomoxir showed a reduced migration and invasion rate. The scale bar is indicated. (**F**) EMT-related proteins were changed correspondingly, and phosphorylated/total AKT was down-regulated. *$P<0.05$, **$P<0.01$, n.s. means no significance. Abbreviation: EMT, epithelial–mesenchymal transition.

in T24 cells (Supplementary Figure S2B). Consistent with the flow cytometry analysis, the Western blot (WB) results showed that G_0/G_1-related proteins such as cyclin D1, CDK2, CDK4, and CDK6 were strongly down-regulated in the low- and high-concentration groups (Figure 4C and Supplementary Figure S2C). Moreover, we detected the upstream indicators of the cell cycle pathway, and found that etomoxir treatment up-regulated p21 and acetyl-p53 proteins in BCa UM-UC-3 cells. Furthermore, the PPARγ-SIRT1 pathway related proteins were analyzed that PPARγ was up-regulated and total and phosphorylated SIRT1 were strongly down-regulated in UM-UC-3 cells (Figure 4C).

Cell migration was detected by wound healing and transwell migration assays. After 12-h incubation, the migration rate of wound healing was calculated in UM-UC-3 cells that the migration rate of etomoxir-treated groups was significantly reduced (Figure 4D). And the transwell migration and invasion assays indicated that etomoxir could decrease the cell invasion and migrations rate of BCa UM-UC-3 (Figure 4E) and T24 cells (Supplementary Figure S2D). In accordance with the transwell assay, WB analysis showed a down-regulation of N-cadherin, Vimentin, β-catenin, Slug, MMP2, and MMP9, and an up-regulation of E-cadherin proteins associated with the epithelial–mesenchymal transition (EMT) process. Furthermore, phosphorylated/total AKT, the upstream regulator of EMT, was down-regulated both in UM-UC-3 (Figure 4F) and T24 cells (Supplementary Figure S2E).

Etomoxir-induced cell cycle arrest was rescued by PPARγ antagonist

Etomoxir, an irreversible inhibitor of CPT1 as reported [25,26], altered the mRNA expression of FAO-related genes in UM-UC-3 cells (Figure 5A). However, we did not observe a significant change of CPT1A both at transcriptional and protein levels (Figure 5A–C). PPARα expression was slightly up-regulated in high-dose group but not
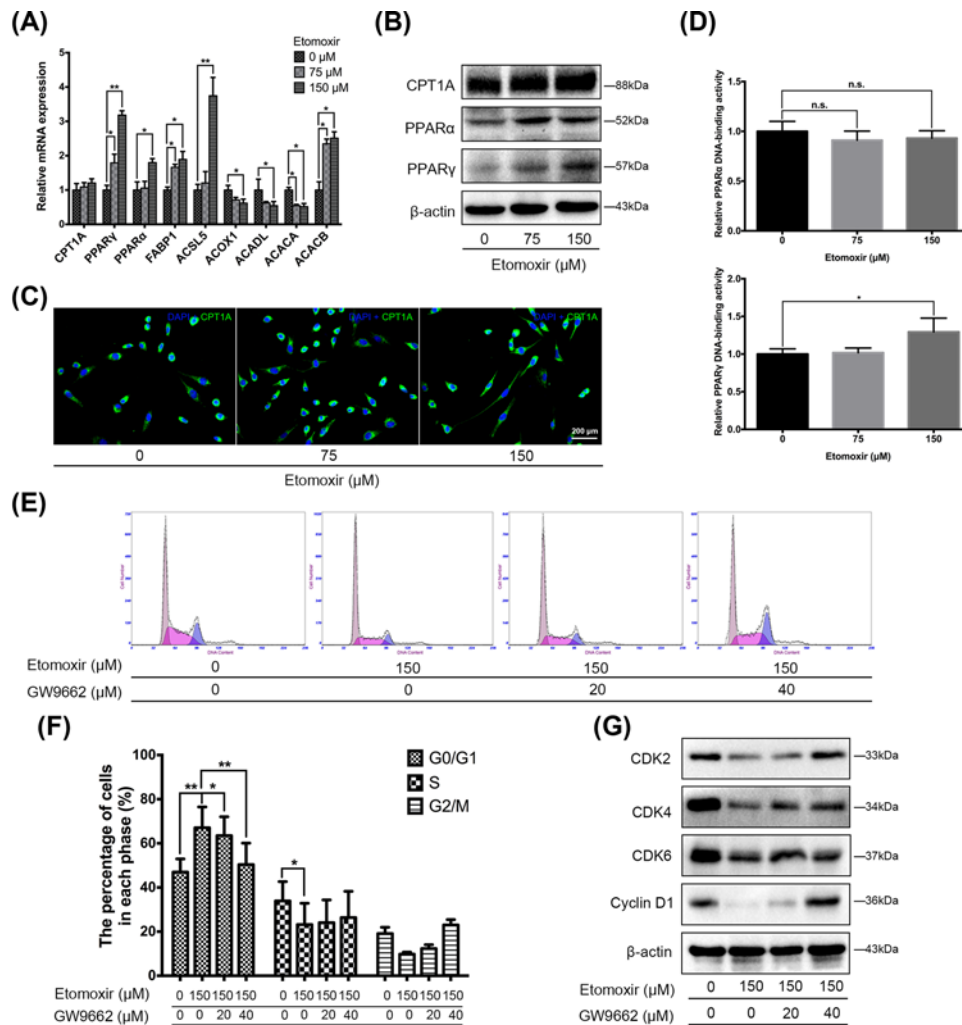
Figure 5. Cell cycle arrest induced by etomoxir was recovered by PPARγ antagonist GW9662 in UM-UC-3 cells
(**A**) Etomoxir treatment regulated the FAO-related gene expressions. (**B**) WB analysis showed that PPARα was slightly increased, and PPARγ was strongly up-regulated. Both the WB analysis and (**C**) IF staining results revealed no significant change in CPT1A. (**D**) ELISA results indicated that etomoxir could increase PPARγ DNA-binding activity in UM-UC-3 when treated with 150 μM, but had no effect on PPARα. (**E**) Flow cytometry analysis revealed that arrested G_0/G_1 cell cycle could be rescued by GW9662, confirmed by statistical analysis (**F**) and the WB results (**G**). The treatment and drug concentrations were indicated. *$P < 0.05$, **$P < 0.01$, n.s. means no significance.

in low-dose group at mRNA level. However, at the protein level, PPARα did not change significantly in both groups (Figure 5B). The results indicated a strong up-regulation of PPARγ expression both at mRNA and protein levels in etomoxir-treated UM-UC-3 cells (Figure 5A,B). The Enzyme-linked immunosorbent assay (ELISA) showed that PPARγ DNA-binding activity was increased in high-dose group compared with the control group in UM-UC-3 cells, but there was no change of PPARα DNA-binding activity (Figure 5D).

Next, we blocked the PPARγ activity with distinct concentrations of PPARγ antagonist GW9662. The flow cytometry analysis showed that the cell cycle G_0/G_1 arrest caused by etomoxir was significantly recovered by GW9662 in a dose-dependent manner in UM-UC-3 (Figure 5E) and T24 cells (Supplementary Figure S2F), confirmed by statistical analysis (Figure 5F and Supplementary Figure S2G). The clonogenic survival assay revealed that GW9662 could partially restore the suppressed proliferation caused by etomoxir (Supplementary Figure S2H–I). Consistently, WB results revealed that the reduced proteins related to G_0/G_1 phase such as CDK2, CDK4, CDK6, and cyclin D1 were also inverted by PPARγ antagonist in BCa UM-UC-3 (Figure 5G) and T24 cells (Supplementary Figure S2J).

Discussion

Reprogramming energy metabolism is considered to be a hallmark of cancer [33]. Otto Warburg first made the point that cancer cells turned to aerobic glycolysis rather than oxidative phosphorylation to sustain the energy supply [34]. However, recent studies have indicated that other substrates such as glutamine and fatty acids are also critical in cancer cell survival, and prostate cancer displays a low rate of glucose utilization and a high rate of fatty acids uptake [18,35]. Moreover, B-cell lymphoma and malignant glioma are highly dependent on FAO for growth and survival [17,36]. Whether the aerobic glycolysis or FAO is predominant in BCa, is still unknown. Related metabolomics analysis and studies revealed that fatty acid metabolism was dysregulated and was promising in treatment and diagnosis of BCa [19,37]. In this study, our microarray and bioinformatics analysis revealed that DEGs between normal bladder and BCa tissues are enriched to lipid metabolism, especially fatty acid metabolism. Genes involved in metabolism were also misregulated in BCa tissues (Supplementary Figure S1A–G). Moreover, KEGG pathway analysis showed that fatty acid degradation was significantly linked to BCa via PPAR signaling pathway. The FFA, which could be transported into mitochondria for oxidation, was also increased in BCa tissues compared with paracancerous tissues (n=9, Figure 1). Thus, on this basis, we hypothesized that FAO was closely related to BCa.

Etomoxir was an inhibitor of FAO, and was developed for treating heart disease and diabetes mellitus for a long time [38,39]. A few studies have reported that etomoxir, which could irreversibly inhibit the function of CPT1, had an influence on CPT1A expression [18]. However, in our study, we did not see the significant change of CPT1A expression at mRNA and protein levels (Figure 5A–C) in BCa cells and *in vivo* experiment (Figure 3D), which might be because of the enzyme activity inhibition rather than the transcriptional regulation of etomoxir. Although recently some studies identified an off-target effect of etomoxir [40,41], still we could see the FAO inhibition of etomoxir in research. Consistently, the FAO inhibition of etomoxir could be validated by increased fatty acid and lipid accumulation and decreased ATP and NADPH level in the present study (Figure 2C–G). Etomoxir could suppress the transportation of long-chain fatty acid into mitochondrial for β-oxidation, thus increasing the level of long-chain fatty acids (Figure 2I). We also observed a significant decrease in C12:0, which might be the compensatory results of long-chain FAO inhibition.

A variety of studies have indicated that reduced ATP by FAO inhibition could suppress tumor cell proliferation. Ricciardi et al. [16] reported that pharmacological inhibition of CPT1A could impair cell proliferation of acute myeloid leukemia. Consistently, our results showed that FAO inhibition by etomoxir could suppress BCa cell growth both *in vitro* (Figure 2A,B,H,K) and *in vivo* (Figure 3). Moreover, we observed an inhibitory effect of etomoxir on invasion and migration, with down-regulated N-cadherin and up-regulated E-cadherin proteins related to EMT, which have been certified to have a critical role in cancer cell invasion and migration [42]. The phosphorylation of AKT at Ser[9] could regulate the EMT pathway [43], which was consistent with our WB results of down-regulated phosphorylated/total AKT (Figure 4F and Supplementary Figure S2E). Furthermore, accumulating studies reported that FAO activation was an important mechanism for tumor cells to develop drug resistance [44]. Galicia-Vazquez et al. [45] reported that ibrutinib-resistant cells of chronic lymphocytic leukemia showed metabolic rewiring to FAO, and FAO inhibition with etomoxir could re-sensitize resistant cells. Intravesical instillations of chemotherapy drugs is an important adjuvant therapeutic method for NMIBC. However, the 5-year recurrence rate and the risk of progression to MIBC is not optimistic [46]. The effect of etomoxir combination with chemotherapy drugs on BCa cells has not been detected. That would be an interesting research subject.

Microarray analysis revealed the connection of BCa with cell cycle and PPAR signaling pathway (Figure 1D). And cell cycle could be blocked at G_0/G_1 phase by etomoxir in BCa UM-UC-3 (Figure 4A) and T24 cells (Supplementary Figure S2A), with changes in G_0/G_1-related proteins (Figure 4C and Supplementary Figure S2C). However, we did not notice a significant change in apoptosis. It might because of the unchanged expression of CPT1A, which could protect cells from apoptosis [47]. CDK inhibitor p21 has been reported as an important tumor suppressor and plays a crucial role in inhibiting cell growth [48]. p53 could induce variable expression of p21 and cyclin D1, which almost exclusively determines the cell cycle status [49]. We observed a strong increase in p21 and acetyl-p53 protein in UM-UC-3 cells when treated with etomoxir. Our previous studies demonstrated the cell cycle regulation of PPARγ-SIRT1 feedback loop in BCa [50]. In this research, we noted an up-regulation of PPARγ and down-regulation of phosphorylated and total SIRT1 in etomoxir-treated UM-UC-3 cell (Figure 4C). We also observed the change of FAO-related gene expression (Figure 5A). Fatty acid synthesis (FAS) was thought to be conflicting with FAO at the same time [51]. But some studies have proved that different isoforms of acetyl-CoA carboxylase, that was ACACA and ACACB, had different subcellular locations and yielded different outcomes of FAO and FAS [21]. It means that FAO and FAS may be active simultaneously and independently in cell and support each other. Simultaneous suppression of FAO and FAS was quite effective in anti-tumor therapy [18,52]. Our results showed a down-regulated expression of ACACA,

PORTLAND
PRESS

which could synthesize malonyl-CoA as substrate for FAS with acetyl-CoA produced by FAO, and an up-regulated expression of ACACB, which could control FAO by producing malonyl-CoA and was reported to be regulated by SIRT1 [53]. Furthermore, after treatment of UM-UC-3 cells with etomoxir, the gene expression and protein level of PPARγ was up-regulated, and the PPARγ DNA-binding activity was also significantly increased. Consequently, we pretreated cells with PPARγ antagonist GW9662 and found that cell cycle arrest induced by etomoxir could be rescued by GW9662. Even though our previous study indicated the anti-tumor effect of GW9662 [54], when PPARγ was pre-inhibited by GW9662, BCa cell proliferation was inhibited to a less degree compared with etomoxir treatment alone (Supplementary Figure S2H-I). In conclusion, our results suggested that FAO inhibition by etomoxir could induce cell cycle arrest at G_0/G_1 phase via PPARγ-mediated pathway.

Multiple types of cancer have been reported to be of the 'lipolytic phenotype', which disobeys the Warburg effect [22,55]. However, the exact metabolic phenotype of BCa still needs to be further explored. Etomoxir was the most commonly used FAO inhibitor and well tolerated in a variety of scientific research, but its clinical trials showed a liver toxicity [27]. The high drug dose might contribute to the undesired side effects. But combined with glutaminolysis or glycolysis and chemotherapy drugs, etomoxir might have a great application prospect. Some other FAO inhibitors like ST1326, a CPT1A-specific inhibitor, also showed significant tumor growth suppression [16,56]. Our findings revealed a novel target and offered a new therapeutic avenue for the treatment of BCa.

Clinical perspectives

- Cancer cells prefer aerobic glycolysis as the main energy source. Recent research highlighted the importance of lipid metabolism in tumor progression and alterations in fatty acid metabolism in BCa. However, there are few studies on fatty acid metabolism especially in BCa.

- Our main findings were that (1) fatty acid metabolism is activated in BCa compared with normal bladder; (2) etomoxir reduced FAO and motility of BCa cells and inhibited cell proliferation *in vitro* and *in vivo*; (3) the cell cycle arrest induced by etomoxir via PPAR-mediated pathway could be recovered by PPAR antagonist.

- Our results revealed that by inhibition of FAO with etomoxir could inhibit tumor cell proliferation and progression in BCa, which may provide a novel avenue to investigate new therapeutic approaches to human BCa.

Ethical statement for human bladder tissues
As described by Cao et al. [30] in our group, the BCa and paracancerous tissues were obtained from patients after surgery at Zhongnan Hospital of Wuhan University, and normal bladder tissues were obtained from donors with accidental death. Tissue samples were collected and stored immediately in liquid nitrogen for the abovementioned experiments. Histological diagnosis of the bladder tissues was confirmed by two pathologists independently. The informed consent was obtained from all subjects and the study was conducted in accordance with the Declaration of Helsinki. The collection and use of human bladder tissues was approved by the Ethics Committee at Zhongnan Hospital of Wuhan University (approval number 2015029).

Competing Interests
The authors declare that there are no competing interests associated with the manuscript.

Author Contribution

S.C., G.W. and X.W. were responsible for conceptualization. S.C. and L.C. were responsible for methodology. Y.W. was responsible for software. Y.X. and X.L. were responsible for validation. L.J. was responsible for formal analysis. K.Q. and L.J. were responsible for resources. G.W. and Y.W. were responsible for data curation. S.C. was responsible for writing-original draft preparation. G.W. and X.L. were responsible for writing-review and editing. X.W. was responsible for supervision. X.W. was responsible for project administration and funding acquisition.

Abbreviations

ATP, adenosine triphosphate; BCa, bladder cancer; CPT1, carnitine palmitoyltransferase I; CPT2, carnitine palmitoyltransferase II; DEG, differentially expressed gene; EMT, epithelial–mesenchymal transition; FAO, fatty acid oxidation; FAS, fatty acid synthesis; FBS, fetal bovine serum; FFA, free fatty acid; GCBI, Gene-Cloud of Biotechnology Information; GO, gene ontology; H&E, Hematoxylin and Eosin; IHC, immunohistochemistry; KEGG, Kyoto Encyclopedia of Genes and Genomes; MIBC, muscle-invasive BCa; NADPH, nicotinamide adenine dinucleotide phosphate; NMIBC, non-muscle-invasive BCa; PFA, paraformaldehyde; PPAR, peroxisome proliferator-activated receptor; WB, Western blot.

References

1   Ferlay, J., Soerjomataram, I., Dikshit, R., Eser, S., Mathers, C., Rebelo, M. et al. (2015) Cancer incidence and mortality worldwide: sources, methods and major patterns in GLOBOCAN 2012. *Int. J. Cancer* **136**, E359–E386, https://doi.org/10.1002/ijc.29210

2   Witjes, J.A., Comperat, E., Cowan, N.C., De Santis, M., Gakis, G., Lebret, T. et al. (2014) EAU guidelines on muscle-invasive and metastatic bladder cancer: summary of the 2013 guidelines. *Eur. Urol.* **65**, 778–792, https://doi.org/10.1016/j.eururo.2013.11.046

3   Prasad, S.M., Decastro, G.J., Steinberg, G.D. and Medscape (2011) Urothelial carcinoma of the bladder: definition, treatment and future efforts. *Nat. Rev. Urol.* **8**, 631–642, https://doi.org/10.1038/nrurol.2011.144

4   Stein, J.P., Lieskovsky, G., Cote, R., Groshen, S., Feng, A.C., Boyd, S. et al. (2001) Radical cystectomy in the treatment of invasive bladder cancer: long-term results in 1,054 patients. *J. Clin. Oncol.* **19**, 666–675, https://doi.org/10.1200/JCO.2001.19.3.666

5   Shabsigh, A., Korets, R., Vora, K.C., Brooks, C.M., Cronin, A.M., Savage, C. et al. (2009) Defining early morbidity of radical cystectomy for patients with bladder cancer using a standardized reporting methodology. *Eur. Urol.* **55**, 164–174, https://doi.org/10.1016/j.eururo.2008.07.031

6   Clark, P.E. (2009) Neoadjuvant versus adjuvant chemotherapy for muscle-invasive bladder cancer. *Expert Rev. Anticancer Ther.* **9**, 821–830, https://doi.org/10.1586/era.09.36

7   Vishnu, P., Mathew, J. and Tan, W.W. (2011) Current therapeutic strategies for invasive and metastatic bladder cancer. *OncoTargets Ther.* **4**, 97–113

8   Gorin, M.A., Ayyathurai, R. and Soloway, M.S. (2012) Diagnosis and treatment of bladder cancer: how can we improve? *Postgrad. Med.* **124**, 28–36, https://doi.org/10.3810/pgm.2012.05.2545

9   Hanahan, D. and Weinberg, R.A. (2011) Hallmarks of cancer: the next generation. *Cell* **144**, 646–674, https://doi.org/10.1016/j.cell.2011.02.013

10 Zhao, Y., Butler, E.B. and Tan, M. (2013) Targeting cellular metabolism to improve cancer therapeutics. *Cell Death Dis.* **4**, e532, https://doi.org/10.1038/cddis.2013.60

11 Bensinger, S.J. and Christofk, H.R. (2012) New aspects of the Warburg effect in cancer cell biology. *Semin. Cell Dev. Biol.* **23**, 352–361, https://doi.org/10.1016/j.semcdb.2012.02.003

12 Koppenol, W.H., Bounds, P.L. and Dang, C.V. (2011) Otto Warburg's contributions to current concepts of cancer metabolism. *Nat. Rev. Cancer* **11**, 325–337, https://doi.org/10.1038/nrc3038

13 Cairns, R.A., Harris, I.S. and Mak, T.W. (2011) Regulation of cancer cell metabolism. *Nat. Rev. Cancer* **11**, 85–95, https://doi.org/10.1038/nrc2981

14 Carracedo, A., Cantley, L.C. and Pandolfi, P.P. (2013) Cancer metabolism: fatty acid oxidation in the limelight. *Nat. Rev. Cancer* **13**, 227–232, https://doi.org/10.1038/nrc3483

15 Hossain, F., Al-Khami, A.A., Wyczechowska, D., Hernandez, C., Zheng, L., Reiss, K. et al. (2015) Inhibition of fatty acid oxidation modulates immunosuppressive functions of myeloid-derived suppressor cells and enhances cancer therapies. *Cancer Immunol. Res.* **3**, 1236–1247, https://doi.org/10.1158/2326-6066.CIR-15-0036

16 Ricciardi, M.R., Mirabilii, S., Allegretti, M., Licchetta, R., Calarco, A., Torrisi, M.R. et al. (2015) Targeting the leukemia cell metabolism by the CPT1a inhibition: functional preclinical effects in leukemias. *Blood* **126**, 1925–1929, https://doi.org/10.1182/blood-2014-12-617498

17 Lin, H., Patel, S., Affleck, V.S., Wilson, I., Turnbull, D.M., Joshi, A.R. et al. (2017) Fatty acid oxidation is required for the respiration and proliferation of malignant glioma cells. *Neuro Oncol.* **19**, 43–54, https://doi.org/10.1093/neuonc/now212.143

18 Schlaepfer, I.R., Rider, L., Rodrigues, L.U., Gijon, M.A., Pac, C.T., Romero, L. et al. (2014) Lipid catabolism via CPT1 as a therapeutic target for prostate cancer. *Mol. Cancer Ther.* **13**, 2361–2371, https://doi.org/10.1158/1535-7163.MCT-14-0183

19 Massari, F., Ciccarese, C., Santoni, M., Iacovelli, R., Mazzucchelli, R., Piva, F. et al. (2016) Metabolic phenotype of bladder cancer. *Cancer Treat. Rev.* **45**, 46–57, https://doi.org/10.1016/j.ctrv.2016.03.005

20 Jin, X., Yun, S.J., Jeong, P., Kim, I.Y., Kim, W.J. and Park, S. (2014) Diagnosis of bladder cancer and prediction of survival by urinary metabolomics. *Oncotarget* **5**, 1635–1645, https://doi.org/10.18632/oncotarget.1744

21 Qu, Q., Zeng, F., Liu, X., Wang, Q.J. and Deng, F. (2016) Fatty acid oxidation and carnitine palmitoyltransferase I: emerging therapeutic targets in cancer. *Cell Death Dis.* **7**, e2226, https://doi.org/10.1038/cddis.2016.132

22 Ma, Y., Temkin, S.M., Hawkridge, A.M., Guo, C., Wang, W., Wang, X.Y. et al. (2018) Fatty acid oxidation: an emerging facet of metabolic transformation in cancer. *Cancer Lett.* **435**, 92–100, https://doi.org/10.1016/j.canlet.2018.08.006

23 Duszka, K., Oresic, M., Le May, C., Konig, J. and Wahli, W. (2017) PPARgamma modulates long chain fatty acid processing in the intestinal epithelium. *Int. J. Mol. Sci.* **18**, 12, https://doi.org/10.3390/ijms18122559

24 Jiang, F., Zhang, Z., Zhang, Y., Wu, J., Yu, L. and Liu, S. (2016) L-carnitine ameliorates the liver inflammatory response by regulating carnitine palmitoyltransferase I-dependent PPARgamma signaling. *Mol. Med. Rep.* **13**, 1320–1328, https://doi.org/10.3892/mmr.2015.4639

25 Bristow, M. (2000) Etomoxir: a new approach to treatment of chronic heart failure. *Lancet* **356**, 1621–1622, https://doi.org/10.1016/S0140-6736(00)03149-4

26 Ratheiser, K., Schneeweiss, B., Waldhausl, W., Fasching, P., Korn, A., Nowotny, P. et al. (1991) Inhibition by etomoxir of carnitine palmitoyltransferase I reduces hepatic glucose production and plasma lipids in non-insulin-dependent diabetes mellitus. *Metabolism* **40**, 1185–1190, https://doi.org/10.1016/0026-0495(91)90214-H

27 Ceccarelli, S.M., Chomienne, O., Gubler, M. and Arduini, A. (2011) Carnitine palmitoyltransferase (CPT) modulators: a medicinal chemistry perspective on 35 years of research. *J. Med. Chem.* **54**, 3109–3152, https://doi.org/10.1021/jm100809g

28 Senni, N., Savall, M., Cabrerizo Granados, D., Alves-Guerra, M.C., Sartor, C., Lagoutte, I. et al. (2019) beta-catenin-activated hepatocellular carcinomas are addicted to fatty acids. *Gu* **68**, 322–334, https://doi.org/10.1136/gutjnl-2017-315448

29 Tan, Z., Xiao, L., Tang, M., Bai, F., Li, J., Li, L. et al. (2018) Targeting CPT1A-mediated fatty acid oxidation sensitizes nasopharyngeal carcinoma to radiation therapy. *Theranostics* **8**, 2329–2347, https://doi.org/10.7150/thno.21451

30 Cao, R., Wang, G., Qian, K., Chen, L., Qian, G., Xie, C. et al. (2017) Silencing of HJURP induces dysregulation of cell cycle and ROS metabolism in bladder cancer cells via PPARgamma-SIRT1 feedback loop. *J. Cancer* **8**, 2282–2295, https://doi.org/10.7150/jca.19967

31 Wang, G., Cao, R., Wang, Y., Qian, G., Dan, H.C., Jiang, W. et al. (2016) Simvastatin induces cell cycle arrest and inhibits proliferation of bladder cancer cells via PPARgamma signalling pathway. *Sci. Rep.* **6**, 35783, https://doi.org/10.1038/srep35783

32 Scholzen, T. and Gerdes, J. (2000) The Ki-67 protein: from the known and the unknown. *J. Cell. Physiol.* **182**, 311–322, https://doi.org/10.1002/(SICI)1097-4652(200003)182:3%3c311::AID-JCP1%3e3.0.CO;2-9

33 Ocana, M.C., Martinez-Poveda, B., Quesada, A.R. and Medina, M.A. (2019) Metabolism within the tumor microenvironment and its implication on cancer progression: an ongoing therapeutic target. *Med. Res. Rev.* **39**, 70–113, https://doi.org/10.1002/med.21511

34 Warburg, O. (1956) On the origin of cancer cells. *Science* **123**, 309–314, https://doi.org/10.1126/science.123.3191.309

35 Lu, W., Pelicano, H. and Huang, P. (2010) Cancer metabolism: is glutamine sweeter than glucose? *Cancer Cell* **18**, 199–200, https://doi.org/10.1016/j.ccr.2010.08.017

36 Monti, S., Savage, K.J., Kutok, J.L., Feuerhake, F., Kurtin, P., Mihm, M. et al. (2005) Molecular profiling of diffuse large B-cell lymphoma identifies robust subtypes including one characterized by host inflammatory response. *Blood* **105**, 1851–1861, https://doi.org/10.1182/blood-2004-07-2947

37 Rodrigues, D., Jeronimo, C., Henrique, R., Belo, L., de Lourdes Bastos, M., de Pinho, P.G. et al. (2016) Biomarkers in bladder cancer: a metabolomic approach using *in vitro* and *ex vivo* model systems. *Int. J. Cancer* **139**, 256–268, https://doi.org/10.1002/ijc.30016

38 Lopaschuk, G.D., Wall, S.R., Olley, P.M. and Davies, N.J. (1988) Etomoxir, a carnitine palmitoyltransferase I inhibitor, protects hearts from fatty acid-induced ischemic injury independent of changes in long chain acylcarnitine. *Circ. Res.* **63**, 1036–1043, https://doi.org/10.1161/01.RES.63.6.1036

39 Wolf, H.P. (1992) Possible new therapeutic approach in diabetes mellitus by inhibition of carnitine palmitoyltransferase 1 (CPT1). *Horm. Metab. Res. Suppl.* **26**, 62–67

40 Raud, B., Roy, D.G., Divakaruni, A.S., Tarasenko, T.N., Franke, R., Ma, E.H. et al. (2018) Etomoxir actions on regulatory and memory T cells are independent of Cpt1a-mediated fatty acid oxidation. *Cell Metab.* **28**, 504.e507–515.e507, https://doi.org/10.1016/j.cmet.2018.06.002

41 Yao, C.H., Liu, G.Y., Wang, R., Moon, S.H., Gross, R.W. and Patti, G.J. (2018) Identifying off-target effects of etomoxir reveals that carnitine palmitoyltransferase I is essential for cancer cell proliferation independent of beta-oxidation. *PLoS Biol.* **16**, e2003782, https://doi.org/10.1371/journal.pbio.2003782

42 van Vuurden, D.G., Aronica, E., Hulleman, E., Wedekind, L.E., Biesmans, D., Malekzadeh, A. et al. (2014) Pre-B-cell leukemia homeobox interacting protein 1 is overexpressed in astrocytoma and promotes tumor cell growth and migration. *Neuro Oncol.* **16**, 946–959, https://doi.org/10.1093/neuonc/not308

43 Ge, H., Liang, C., Li, Z., An, D., Ren, S., Yue, C. et al. (2018) DcR3 induces proliferation, migration, invasion, and EMT in gastric cancer cells via the PI3K/AKT/GSK-3beta/beta-catenin signaling pathway. *OncoTargets Ther.* **11**, 4177–4187, https://doi.org/10.2147/OTT.S172713

44 Farge, T., Saland, E., de Toni, F., Aroua, N., Hosseini, M., Perry, R. et al. (2017) Chemotherapy-resistant human acute myeloid leukemia cells are not enriched for leukemic stem cells but require oxidative metabolism. *Cancer Discov.* **7**, 716–735, https://doi.org/10.1158/2159-8290.CD-16-0441

45 Galicia-Vazquez, G. and Aloyz, R. (2018) Ibrutinib resistance is reduced by an inhibitor of fatty acid oxidation in primary CLL lymphocytes. *Front. Oncol.* **8**, 411, https://doi.org/10.3389/fonc.2018.00411

46 Sylvester, R.J., van der Meijden, A.P., Oosterlinck, W., Witjes, J.A., Bouffioux, C., Denis, L. et al. (2006) Predicting recurrence and progression in individual patients with stage Ta T1 bladder cancer using EORTC risk tables: a combined analysis of 2596 patients from seven EORTC trials. *Eur. Urol.* **49**, 466–465, https://doi.org/10.1016/j.eururo.2005.12.031

47 Grosch, S., Schiffmann, S. and Geisslinger, G. (2012) Chain length-specific properties of ceramides. *Prog. Lipid Res.* **51**, 50–62, https://doi.org/10.1016/j.plipres.2011.11.001

48 Sherr, C.J. and Roberts, J.M. (1999) CDK inhibitors: positive and negative regulators of G1-phase progression. *Genes Dev.* **13**, 1501–1512, https://doi.org/10.1101/gad.13.12.1501

49 Yang, H.W., Chung, M., Kudo, T. and Meyer, T. (2017) Competing memories of mitogen and p53 signalling control cell-cycle entry. *Nature* **549**, 404–408, https://doi.org/10.1038/nature23880

50 Cao, R., Wang, G., Qian, K., Chen, L., Ju, L., Qian, G. et al. (2018) TM4SF1 regulates apoptosis, cell cycle and ROS metabolism via the PPARgamma-SIRT1 feedback loop in human bladder cancer cells. *Cancer Lett.* **414**, 278–293, https://doi.org/10.7150/jca.19967

51 McGarry, J.D., Mannaerts, G.P. and Foster, D.W. (1977) A possible role for malonyl-CoA in the regulation of hepatic fatty acid oxidation and ketogenesis. *J. Clin. Invest.* **60**, 265–270, https://doi.org/10.1172/JCI108764

52 Tirado-Velez, J.M., Joumady, I., Saez-Benito, A., Cozar-Castellano, I. and Perdomo, G. (2012) Inhibition of fatty acid metabolism reduces human myeloma cells proliferation. *PLoS ONE* **7**, e46484, https://doi.org/10.1371/journal.pone.0046484

53 Corbet, C., Pinto, A., Martherus, R., Santiago de Jesus, J.P., Polet, F. and Feron, O. (2016) Acidosis drives the reprogramming of fatty acid metabolism in cancer cells through changes in mitochondrial and histone acetylation. *Cell Metab.* **24**, 311–323, https://doi.org/10.1016/j.cmet.2016.07.003

54 Cheng, S., Qian, K., Wang, Y., Wang, G., Liu, X., Xiao, Y. et al. (2019) PPARgamma inhibition regulates the cell cycle, proliferation and motility of bladder cancer cells. *J. Cell. Mol. Med.* **23**, 3724–3736, https://doi.org/10.1111/jcmm.14280

55 Liu, Y. (2006) Fatty acid oxidation is a dominant bioenergetic pathway in prostate cancer. *Prostate Cancer Prostat. Dis.* **9**, 230–234, https://doi.org/10.1038/sj.pcan.4500879

56 Pacilli, A., Calienni, M., Margarucci, S., D'Apolito, M., Petillo, O., Rocchi, L. et al. (2013) Carnitine-acyltransferase system inhibition, cancer cell death, and prevention of myc-induced lymphomagenesis. *J. Natl. Cancer Inst.* **105**, 489–498, https://doi.org/10.1093/jnci/djt030